Engineering

Electrical Engineering fields

Okayama University   *Year* 1991

A single-phase PWM AC to DC converter with a step up/down voltage and sinusoidal source current

Shigeyuki Funabiki   Noriyuki Toita
Okayama University   Okayama University

Abdallah Mechi
Okayama Univeristy

A Single-Phase PWM AC to DC Converter
with a Step up/down Voltage and Sinusoidal Source Current

Shigeyuki FUNABIKI, Noriyuki TOITA & Abdallah MECHI

Dept. of Electrical & Electronic Engineering

Okayama University, Okayama 700 Japan

Abstract - A new pulse width modulation (PWM) AC to DC converter is proposed for a variable DC voltage supply. This converter has an advantage of controlling the DC voltage from zero to more than the maximum value of the AC source voltage and having a sinusoidal source current. The input characteristics and the control characteristics of DC voltage are clarified by the computer simulation and they are confirmed by the experiment using a microprocessor-based control system. Further, the dynamic characteristics are discussed by simulation and experiment.

I. INTRODUCTION

The PWM inverter with a fixed pulse pattern in combination with a pulse amplitude modulation (PAM) is useful for the improvement of its output voltage waveform [1,2]. Therefore, it is necessary to develop a variable DC voltage power supply. In general, the DC voltage is obtained by rectifying the AC voltage. However, the AC to DC converter using thyristors has low input power factor and much generation of the lower-order harmonics. Then, it is desirable to develop the variable DC voltage power supply with a high input power factor for the realization of the power converter with combination of PAM and PWM.

The AC to DC converter with a high input power factor has been proposed for the variable DC voltage supply [3]. The controllable region of DC voltage in this converter is less than the maximum value of the AC source voltage. Then, the authors also proposed a new AC to DC converter with a high input power factor [4]. The controllable region of DC voltage is expanded to more than the maximum value of the AC source voltage. Furthermore, the modified PWM control strategy of this AC to DC converter was proposed for the improvement of the displacement power factor [5].

In this paper, the PWM AC to DC converter with two switching devices is proposed and its control characteristics are discussed by simulation and experiment. The PWM strategy of the proposed AC to DC converter is based on the equalizing area method [6]. Then, the steady state characteristics and the dynamic performance of the converter

characteristics and the dynamic performance of the converter are discussed by the computer simulation. These results are confirmed by the experiment using a microprocessor-based control system.

II. AC TO DC CONVERTER AND ITS BEHAVIOR

AC to DC Converter

Fig. 1 shows a single-phase PWM AC to DC converter. The circuit is composed of a diode bridge with two switches, a reactor in a DC link, a series connection of a diode and a capacitor parallel to a load, and an input filter. The proposed converter is an application of the step-up/down chopper to an AC to DC converter.

Behavior of Converter

The performance of the converter is the same in the positive half cycle and in the negative half cycle of the AC source voltage. Then, the switch S_{W1} acts in the positive half cycle of the AC source voltage and the switch S_{W2} acts in the negative half cycle based on the PWM strategy described in the next chapter. The harmonics produced in the converter are filtered and then the source current becomes a quasi-sinusoidal waveform.
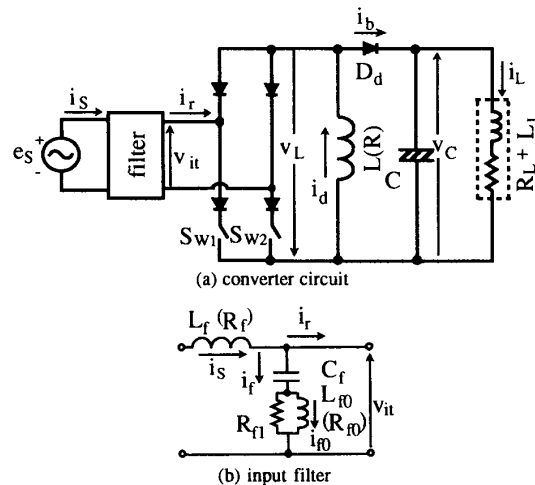

(a) converter circuit

(b) input filter

Fig. 1 Single-phase PWM AC to DC converter

III. VOLTAGE CONTROL AND PWM STRATEGY

Voltage Control

The DC voltage of the PWM AC to DC converter is controlled by regulating the current command every half cycle of the AC source. Then, the current command in the m-th half cycle is decided by the digital PI control. Therefore, the current command is calculated by

$$I_S^*(mT) = I_S^*(mT-T) + K_P[e(mT) - e(mT-T)] + K_I e(mT) \quad (1)$$

$$e(mT) = V_C^*(mT) - \overline{V_C}(mT) \quad (2)$$

where,

$I_S^*(mT)$ r.m.s. value of current command in the m-th half cycle

T time of half cycle

K_P, K_I gains of proportional control and integral control

$V_C^*(mT)$ voltage command in the m-th half cycle

$\overline{V_C}(mT)$ average value of DC voltage in the m-the half cycle

PWM Strategy

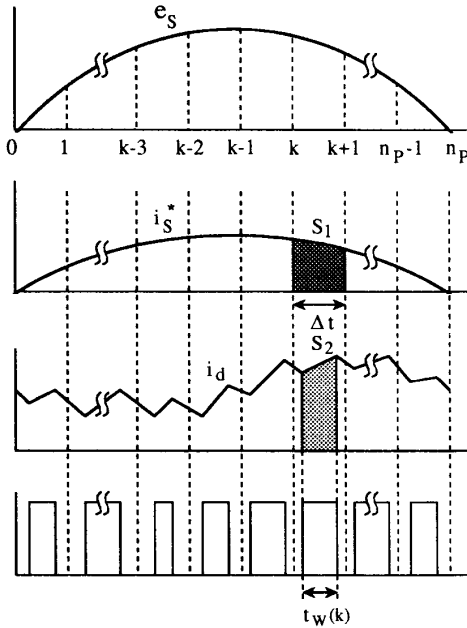Fig. 2 shows the method of deciding the on-time of switch. The half cycle of the AC source voltage is divided

Fig. 2 Decision of on-time of switch

into n_P equal periods. One period Δt is $1/(2n_P f_S)$, where f_S is the frequency of the AC source. The current command $i_S^*(t)$ is expressed by

$$i_S^*(t) = \sqrt{2} \; I_S^*(mT) \sin(\omega_S t) \quad (3)$$

where,

ω_S angular frequency of AC source

Then, the area S_1 in Fig. 2 is obtained by

$$S_1 = \int_{(k-1)\Delta t}^{k\Delta t} i_S^*(t) dt$$

$$= \overline{i_S^*}(k) \, \Delta t \quad (4)$$

where,

$\overline{i_S^*}(k)$ average value of current command in the k-th period

On the other hand, the area S_2 is calculated by

$$S_2 = \frac{i_d(k-1) + i_d(k)}{2} t_W(k) \quad (5)$$

where,

$i_d(k-1)$ detected value of DC reactor current at the (k-1)th point

$i_d(k)$ predicted value of DC reactor current at the k-th point

$t_W(k)$ on-time of switch

Then, $i_d(k)$ is predicted by

$$i_d(k) = i_d(k-1) + \frac{1}{L} [\overline{e_S}(k) t_W(k) - \overline{v_C}(k)\{\Delta t - t_W(k)\}] \quad (6)$$

where,

$\overline{e_S}(k)$ average value of AC source voltage in the k-th period

$\overline{v_C}(k)$ average value of DC voltage in the k-th period

L inductance of DC reactor

The on-time of switch is calculated every period by equalizing S_1 to S_2. Therefore, we obtain the on-time of switch $t_W(k)$ in the k-th period by

$$t_W(k) = \frac{-b + \sqrt{b^2 + 4ac}}{2a} \quad (7)$$

where,

$$a = \frac{1}{2L} \{\overline{e_S}(k) + \overline{v_C}(k)\}$$

$$b = i_d(k\text{-}1) - \frac{\overline{v_C}(k)\Delta t}{2L}$$

$$c = \overset{*}{\overline{i_S}}(k)\Delta t$$

It takes long time to calculate the on-time of switch in eq.(7). Therefore, eq.(7) is approximated in the next equation by using the binomial theorem.

$$t_W(k) = \frac{c}{b} \tag{8}$$

Prediction of Current and Voltage

The calculation of the on-time of switch in the k-th period is executed in the (k-1)th period. The value of the DC reactor current and the average value of the DC voltage in the k-th period are necessary at this time. Therefore, the next predictions are introduced for calculating the on-time of switch.

$$i_d(k\text{-}1) = 2i_d(k\text{-}2) - i_d(k\text{-}3) \tag{9}$$

$$\overline{v_C}(k) = v_C(k\text{-}2) \tag{10}$$

where,

$i_d(k\text{-}2)$, $i_d(k\text{-}3)$ values of DC reactor current at the (k-2)th
  and (k-3)th points

$v_C(k\text{-}2)$ value of output voltage at the (k-2)th point

Then, the next assumption is introduced for the average value of the current command in the k-th period of the m-th half cycle.

$$\overset{*}{\overline{i_S}}(k) = \sqrt{2}\ \overset{*}{I_S}(mT) \sin\{\omega_S(k\text{-}0.5)\Delta t\} \tag{11}$$

IV. SIMULATION METHOD AND EXPERIMENTAL SYSTEM

Simulation Method

The analysis of operating modes is carried out for the simulation. Then, we have five operating modes in the positive half cycle as shown in Fig. 3. Denoting the currents and the voltages as shown in Fig. 1, the state conditions in each mode are shown in Table 1. The circuit equations of the PWM AC to DC converter are expressed in a matrix form by

$$\dot{X}_j(t) = A_j X_j(t) + B_j u_j(t) \tag{12}$$

where,

$X_j(t)$ state vector in mode j (j=1,2,3,4,5)

$u_j(t)$ input vector in mode j

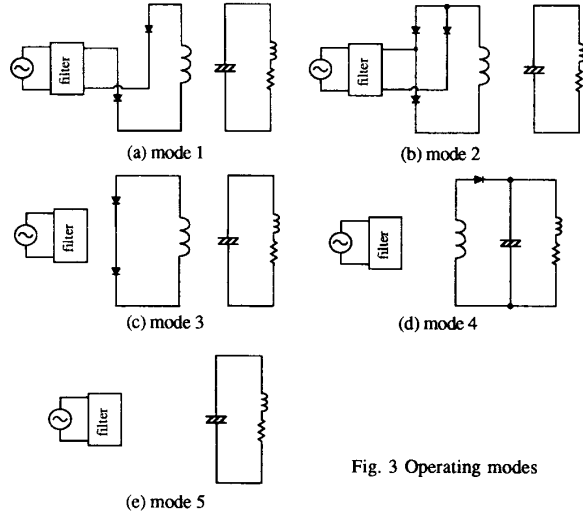A_j, B_j A matrix and B matrix in mode j

(a) mode 1   (b) mode 2

(c) mode 3   (d) mode 4

(e) mode 5

Fig. 3 Operating modes

Table 1 Condition of each operating mode

mode	conditions
1	$i_b(t) = 0$, $i_d(t) = i_r(t)$, $v_L(t) = v_{it}(t)$
2	$i_S(t) = i_r(t)$, $i_b(t) = 0$, $v_{it}(t) = 0$, $v_L(t) = 0$
3	$i_r(t) = 0$, $i_b(t) = 0$, $v_L(t) = 0$
4	$i_r(t) = 0$, $v_L(t) = - v_C(t)$, $i_d(t) = i_b(t)$
5	$i_r(t) = 0$, $i_d(t) = 0$, $i_b(t) = 0$, $v_L(t) = 0$

Then, eq.(12) is rewritten in the discrete state equation. The digital simulation is implemented for the discussion of the performance of the proposed PWM AC to DC converter.

Experimental System

Fig. 4 shows the experimental system of the proposed PWM AC to DC converter by using a microcomputer. The Intel 80286 microprocessor is used for a CPU in the control
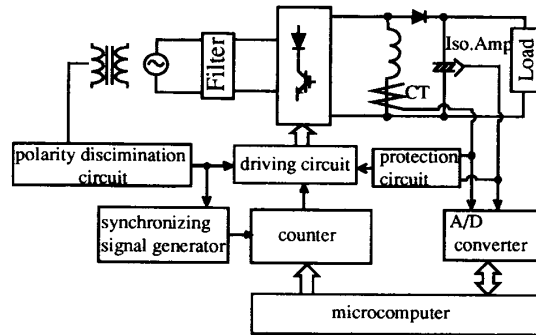

Fig. 4 Experimental system

system. The switching devices used in the experiment are IGBTs.

The DC reactor current is detected through the current transformer (CT) and the output voltage is detected through the isolation amplifier (Iso. Amp.). Then, the microcomputer calculates the on-time of switch and drives the switching devices through the driving circuit.

V. CONTROL CHARACTERISTICS

Steady State Characteristics

Fig. 5 shows the voltage and current waveforms in the experiment and the simulation. The circuit constants and conditions are listed in Table 2. The DC reactor is 50 mH with a quality factor of 100 and the output capacitor is 1000
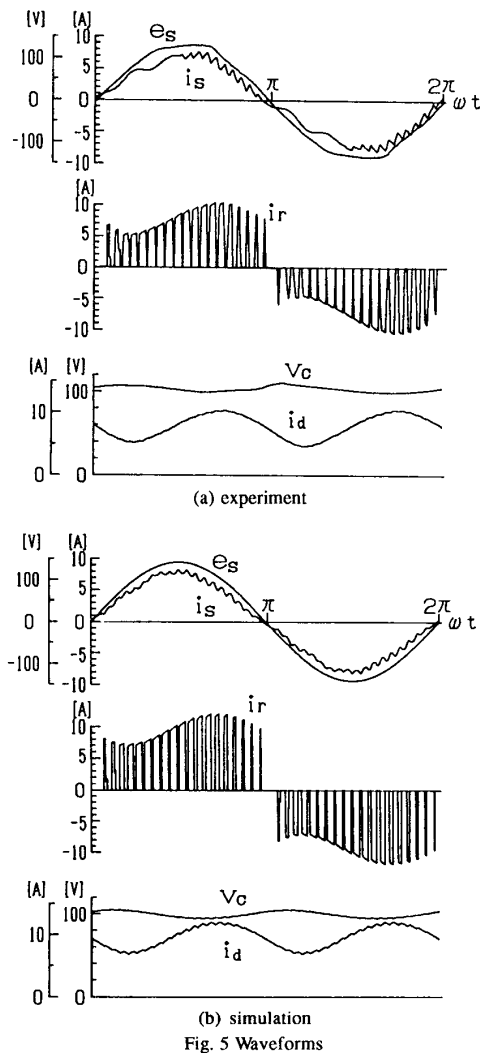
Table 2 Circuit constants and condition

AC source	E_S	100.0 V
	f_S	60.0 Hz
Input filter	L_f	6.0 mH
	R_f	0.1 Ω
	C_f	10.0 μF
	L_{f0}	2.2 mH
	R_{f0}	0.083 Ω
	R_{f1}	7.3 Ω
Load	R_L	30.0 Ω
	L_L	10.0 mH
Division of half cycle n_p		20

μF. The current command is 5.0 A. The waveforms in the simulation agree well with those in the experiment. The DC reactor current has a large ripple due to the rectifying operation. The source current is, however, in phase with the AC source voltage and a quasi-sinusoidal waveform.

Fig. 6 shows the input characteristics of the PWM AC to DC converter with the output capacitor of 1000 μF. The distortion factor DF is expressed by

(a) experiment

(b) simulation

Fig. 5 Waveforms

(a) distortion factor

(b) input power factor

Fig. 6 Input characteristics
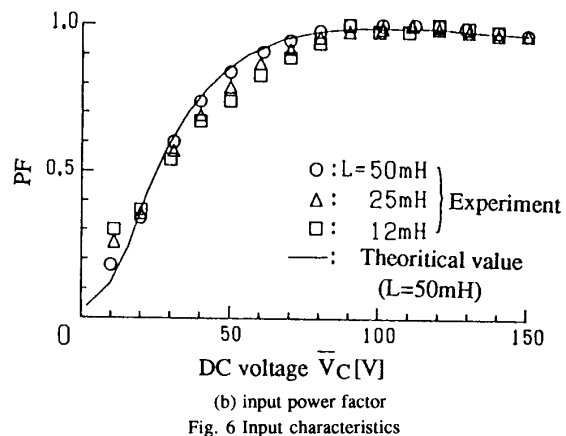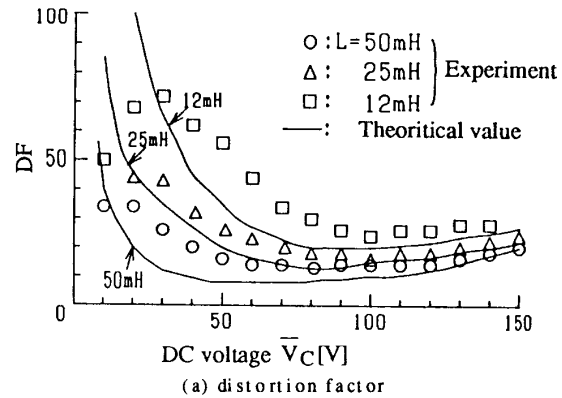
$$DF = \frac{\sqrt{\sum\limits_{n=2}^{\infty} I_n^2}}{I_1} \qquad (13)$$

where,

I_n n-th harmonic of AC source current

The input power factor PF is expressed in the next equation.

$$PF = \frac{1}{\sqrt{1+DF^2}} \cos(\phi_1) \qquad (14)$$

where,

$\cos(\phi_1)$ displacement power factor

DF becomes smaller as the DC reactor becomes larger. That is because the ripple in the DC reactor current becomes smaller. Further, DF becomes larger as the DC voltage becomes smaller. That is because there are errors in the calculation of pulse width by eq.(8) and the pulse width is saturated due to small DC reactor current.

PF is nearly an unity above the DC voltage of 80 V. However, PF drops rapidly under 50 V. Because $\cos(\phi_1)$ rapidly becomes smaller due to the leading filter current.

Fig. 7 shows the control characteristics of DC voltage. The circuit constants and conditions are listed in Table 2 and the DC reactor is 50 mH with a quality factor of 100. The output capacitor is 1000 µF. The DC voltage obtained in the experiment agrees well with the DC voltage command. However, the experimental results in the small range of DC voltage are a little larger than the theoretical ones due to the errors in the approximation of $t_w(k)$ by eq.(8).

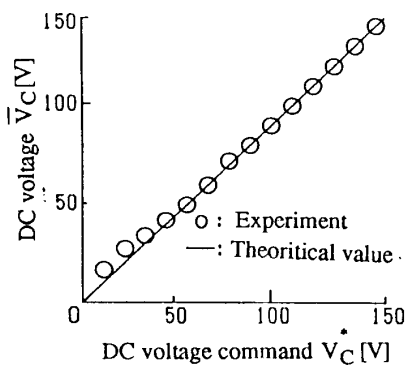Fig. 8 shows the ripple factor of DC voltage. The ripple factor is expressed by
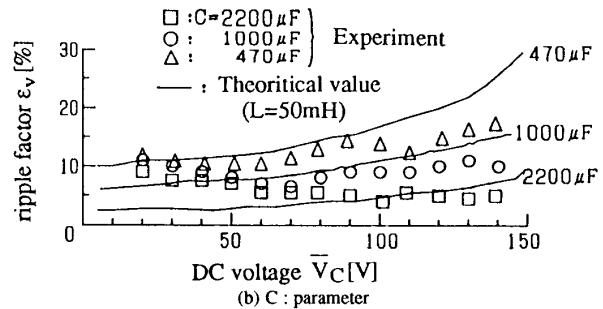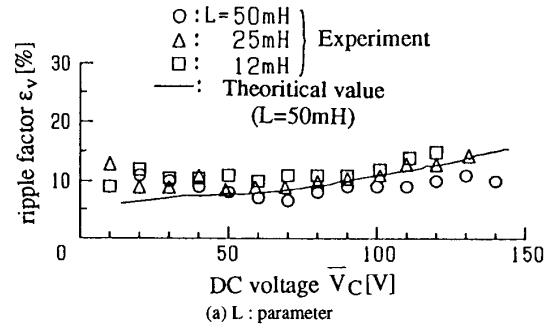

Fig. 7 Control characteristics of DC voltage

(a) L : parameter

(b) C : parameter

Fig. 8 Ripple factor of DC voltage

$$\varepsilon_V = \frac{V_{Cmax} - V_{Cmin}}{\overline{V_C}} \times 100 \qquad (15)$$

where,

V_{Cmax} maximum value of DC voltage

V_{Cmin} minimum value of DC voltage

$\overline{V_C}$ average value of DC voltage

The output capacitor is 1000 µF in Fig. 8(a) and the DC reactor is 50 mH in Fig. 8(b). ε_V becomes smaller as the output capacitor becomes larger and the DC voltage becomes smaller.

Dynamic Performance

Fig. 9 shows the response for the step change of DC voltage command from 70 V to 110 V in the experiment and the simulation. The circuit constants and conditions are listed in Table 2 and the inductance of DC reactor is 50 mH with a quality factor of 100, and the output capacitor is 1000 µF. Then, the gains K_P and K_I of the PI controller are 0.05 and 0.025, respectively. These gains are decided for a good response by the simulation.

The simulated response of the DC voltage agrees well with the experimental one. The DC voltage follows well the step change of DC voltage command and its response time is about two and half cycles. The DC reactor current and the AC

(a) experiment

(b) simulation

Fig. 9 Dynamic characteristics

AC to DC converter is very available for the variable DC voltage supply.

REFERENCES

(1) I. Takahashi & H. Mochikawa : " Optimum PWM Waveforms of an Inverter for Decreasing Acoustic Noise of an Induction Motor ", IEEE Trans. Ind. Applic., Vol.IA-22, No.5, p.828 1986

(2) Yoon-Jong Lee, Ki-Young Suh & Dong-Wha Chung : " Optimal PAWM strategy for variable speed drive of three phase induction motor ", Trans. Korea Inst. Electr. Eng. (South Korea), Vol.36, No.9, p.616 1987

(3) R. Itoh : " Steady-state and transient characteristics of a single-way step-down PWM GTO voltage-source converter with sinusoidal supply currents ", Proc. IEE, Vol.136, Pt.B, No.4, p.168 198

(4) S. Funabiki & S.Matsuo: " Analysis of a PWM Controlled AC to DC Converter with a Controllability of DC Voltage and a High Input Power Factor ", 1990 IPEC Tokyo Conference Record, Vol.1, p.505

(5) S. Funabiki : " A Single-Phase PWM Controlled AC to DC Converter Based on Control of Unity Displacement Power Factor ", IEEE 1990 IAS Annual Meeting Record, Part II, p.1012

(6) S. Funabiki : " A Control Strategy of Three-Phase PWM Inverter with Fluctuating Input Voltage ", IEEE IAS 1989 Annual Meeting Record, Part I, p.1170 1989
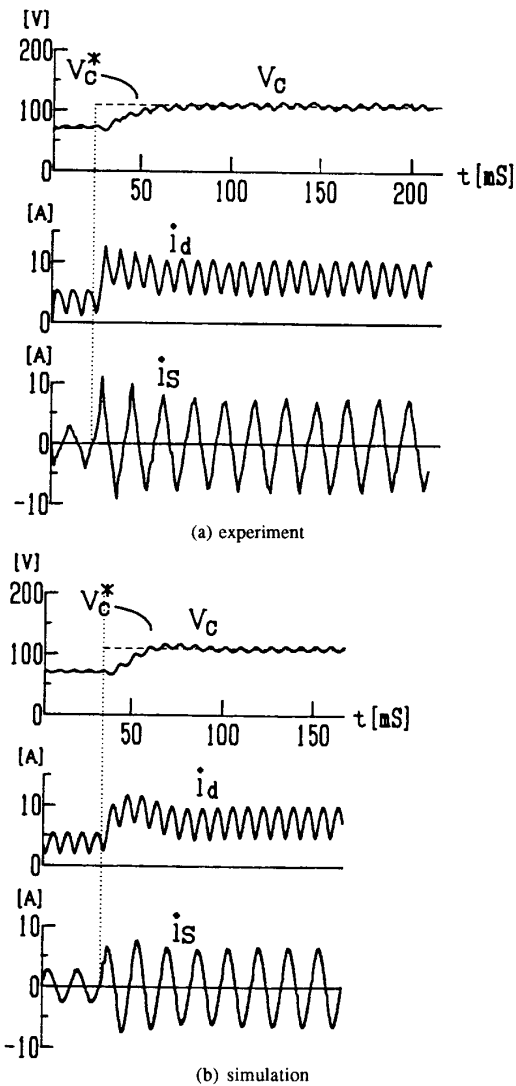
source current become large in the several half cycles after the change of DC voltage command due to the energy storage in the DC reactor. After then, the current and the voltage of the PWM AC to DC converter become in steady state.

VI. CONCLUSIONS

The new PWM AC to DC converter is proposed with a wide range of DC voltage and a sinusoidal source current. The steady state characteristics and the dynamic performance of the PWM AC to DC converter are discussed by the digital simulation and the experiment using the microprocessor-based control system. It is clarified that this proposed PWM